Applications and Applied Mathematics: An International Journal (AAM)

Volume 19
Issue 3 *Special Issue No. 12 (March 2024)*

Article 8

3-2024

Effects of Magnetic Field and Chemical Reaction on a Time Dependent Casson Fluid Flow

Akhil Mittal
Government Science College

Harshad Patel
Ganpat University

Ramesh Patoliya
Gujarat Technological University

Vimalkumar Gohil
GEC-Bhavnagar

Available at
http://pvamu.edu/aam
Appl. Appl. Math.
ISSN: 1932-9466

Applications and Applied Mathematics:
An International Journal
(AAM)

Special Issue No. 12 (March 2024), Article 8, 12 pages

Effects of Magnetic Field and Chemical Reaction on a Time Dependent Casson Fluid Flow

[a]Akhil Mittal, [b*]Harshad Patel, [c]Ramesh Patoliya, [d]Vimalkumar Gohil

[a] Government Science College
Santrampur, India
akhilsmittal@gmail.com

[b*] U. V. Patel College of Engineering
Ganpat University, Kherva
harshadpatel2@gmail.com

[c] Research Scholar, KSET-KPGU
Gujarat Technological University,
Ahmedabad
rkpatoliya@gmail.com

[d] GEC-Bhavnagar
vpgohil0909@gmail.com

*Corresponding author

Received: May 1, 2023; Accepted: December 10, 2023

Abstract

This research paper deals with the effect of chemical reactions and magnetic fields on the hydrodynamics fluid flow of Casson fluid. The novelty of this work is the inclusion of time-dependent flow across a vertical plate with a stepped concentration at the surface in a porous media. The stated phenomenon is modeled in the PDE system and is adapted in the ODE system through similarity transformation. The LT (Laplace Transform) and ILT (Inverse LT) are used to obtain the analytical results for regulating dimension-free movement, thermals, and concentration expression. The exact expression of shear rate, heat exchange rate, and mass exchange rate are obtained. The consequences of different tangible parameters in proposed problems were presented by diagrams. From the result, it is concluded that velocity profiles are delayed with rising the number of magnetic fields. It can be analyzed that temperature is enhanced with thermal radiation, whereas concentration profiles are delayed with chemical reaction parameters.

Keywords: M.H.D. flow; Porous medium; Chemical reaction; Shear rate; Heat exchange rate; Mass transfer rate

MSC 2010 (or 2020) No.: 76W05, 35N30, 35Q30

Terminology

u	Velocity $(m\, s^{-1})$
T	Heat transfer (k)
C	Mass transfer $(Kg\, m^{-3})$
C_p	Specific heat $(JKg^{-1}k)$
D	Diffusivity of Mass $(\, m^2 s^{-1})$
Pr	Prandtl Number
Gm	Grashof number of Concentration.
Gr	Grashof number of Temperature.
t	Time (s)
Kr	Chemical Reaction
Sc	Schmidt number
γ	Casson parameter
σ	Electric conductivity $(m^{-1}s)$
ρ	Density $(Kg\, m^{-3})$
k	Thermal conductivity $(\, W\, m^{-1}k^{-1})$
ν	Kinematic viscosity $(m^2 s^{-1})$
φ	Porosity
$\mu\beta$	Dynamic viscosity $(m^2 s^{-1})$

1. Introduction

As we know, Magnetohydrodynamics (MHD) is a widely used topic in engineering and physical science for practical and basic research today. Hartmann (1937) observed that the laminar flow of liquid is a conductor of electricity under the region of homogeneous magnetism.

The use of a non-Newtonian fluid in engineering is becoming more important due to its rising importance. Casson fluid is a fluid that does not change with time, and it is non-Newtonian as well. This fluid is well-known for its unique properties. The fluid model by Casson (1957) proposed a method for estimating the flow characteristics of mixtures of pigments and oils. Analytic resolution for the unstable free convective MHD flow of Nano fluid was derived by Kataria and Mittal (2015). Rajput et al. (2016) have done remarkable work on Hall-current effects on unsteady MHD flow. Ramesh et al. (2018) have studied radiation enhancement on MHD Casson-fluid flow along an extended tube with a liquid-particle mixture. That proves that MHD flow is critical for a variety of scientific and engineering applications. It has practical uses in the removal of heat from nuclear fuel, fragments, subsurface waste material handling, which is radioactive, food storage, the production of paper, the exploration of oil, etc.

That can be stated scientifically that the MHD free convection is an unreliable Casson-fluid flow. A Casson liquid model was also analyzed by Divya et al. (2020). Radiation absorption and thermal generation/absorption through an endless vertical porous sheet with infinitely accelerated were studied by Rao et al. (2020). Deo et al. (2021) observed the Liquid flow model MHD Reiner-Rivlin via a porous cylindrical annulus. Vaddemani et al. (2021) studied the MHD movement of Casson fluid via a vertical plate that is angled. Rajput et al. (2021) considered different physical effects like hall current and thermal radiation on hydrodynamics flow. Reddy et al. (2022) discussed the MHD flow of Casson with heat generation effects, which is past an oscillating vertical plate. Recently, Krishna (2022) and Prameela et al. (2022) considered the free convective flow of Casson fluid.

The novelty of this work is to find a mathematical expression for natural convective Casson fluid will MHD flow that is unsteady. This includes flow on a vertical plate that accelerates exponentially under the radiation effect in a porous medium. This research has a diverse set of uses in the dying industry and petroleum products.

2. Mathematical formulation

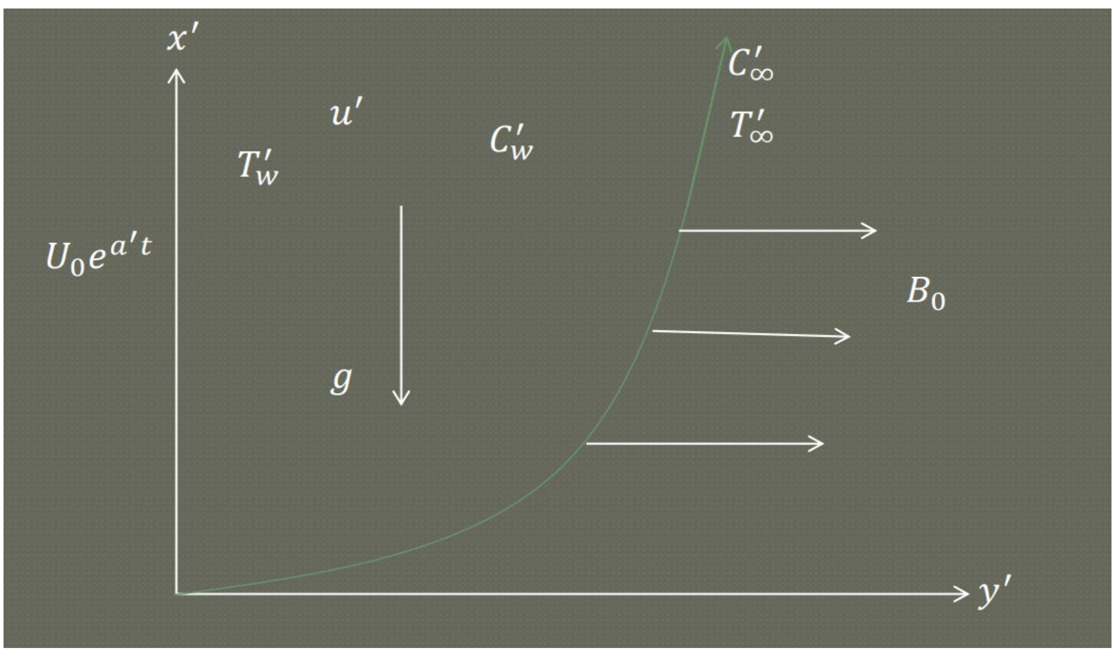

Figure 1. Physical sketch

Figure 1 shows that the $x' - axis$ in an upward way and $y' - axis$ is perpendicular to the wall. A homogeneous magnetic zone of power B_0 in the flow direction is applied, as shown in Sketch. Originally, when duration $t' \leq 0$, the sheet as well as the liquid will remain at a halt and maintain a steady temperature - say T'_∞ and the constant density – say C'_∞. When time $t' > 0$, the plate is exponentially accelerated in the vertical direction; against the gravitational field having velocity $U_0e^{a't}$. The heat of the plate is controlled at a consistent level at T'_w with the rate of volume transmission near the surface of the wall, which is increased/decreased by $C'_\infty +$

$(C_w' + C_\infty')\frac{t'}{t_0}$, when $t' \leq t_0$. When $t' > t_0$, it remained consistent surface concentration C_w' respectively.

The Casson fluid's constitutive equation can be expressed as:

$$\tau_{ij} = \begin{cases} 2\left(\mu B + \frac{Py}{\sqrt{2\pi}}\right) e_{ij}; \pi > \pi_c \\ 2\left(\mu B + \frac{Py}{\sqrt{2\pi_c}}\right) e_{ij}; \pi < \pi_c \end{cases}, \tag{1}$$

Here $\pi = e_{ij}e_{ij}$ with $e_{ij} = (i,j)^{th}$ section as a percentage of deformation, π_c denotes the key value of π according to a format that is non-Newtonian, μB is plastic viscosity in a dynamic state and P_y denotes fluid yield stress.

The "Solid surface," "flow is not compressible," "single dimensional flow," and "fluid is non-Newtonian" are the assumed terms. "Naturally dissipation," "magnetization elicitation," "electric region," and "phrase for variable viscosity" are ignored for the energy equation. If the approximation of Boussinesq is applied with the presumption stated above, the regulating formulas will be found which are as below:

$$\rho \frac{\partial u^{'}}{\partial t^{'}} = \mu_B\left(1 + \frac{1}{\gamma}\right)\frac{\partial^2 u^{'}}{\partial y^2} - \sigma B_0^2 u^{'} - \frac{\mu\varphi}{k_1^{'}} u^{'} + \rho g \beta_T^{'}\left(T^{'} - T_\infty^{'}\right) + \rho g \beta_C^{'}\left(C^{'} - C_\infty^{'}\right), \tag{2}$$

$$\frac{\partial T^{'}}{\partial t^{'}} = \frac{k}{\rho c_p}\frac{\partial^2 T^{'}}{\partial y^{'2}} - \frac{1}{\rho c_p}\frac{\partial q_r}{\partial y^{'}}, \tag{3}$$

$$\frac{\partial C'}{\partial t'} = D_M \frac{\partial^2 C'}{\partial y'^2} - k_2'\left(C' - C_\infty^{'}\right). \tag{4}$$

Having the beginning and termination constraints:

$$u' = 0, T' = T_\infty', C' = C_\infty'; \text{ As } y' \geq 0 \text{ and } t' \leq 0,$$

$$u' = U_0 e^{a't}, T' = T_w', C' = \begin{cases} C_\infty' + (C_w' - C_\infty')\frac{t'}{t_0}, 0 < t' < t_0 \\ C_w',\ t' \geq t_0, t' > 0 \end{cases}, y' = 0,$$

$$u' \to 0, T' \to T_\infty' \ \& \ C' \to C_\infty' \text{ as } y' \to \infty \text{ and } t' \geq 0. \tag{5}$$

Using Brewster (1972), the heat flux of radiative term can be written as:

$$q_r{}' = -\frac{4\sigma^*}{3k^*}\frac{\partial T'^4}{\partial y'}, \tag{6}$$

where $\sigma^* -$ Stefan Boltzmann and $k^* -$ Coefficient of absorption. Considering that the gap between the temperature of the liquid near the coat and the remaining liquid is small, hence T'^4 can be expressed using the Taylor's series expansion at T_∞ where the higher-order term is neglected,

$$T'^4 \cong 4T_\infty'^3 T' - 3T_\infty'^4. \tag{7}$$

As a result,

$$\frac{\partial q_r{}'}{\partial y'} = -\frac{16\sigma^* T_\infty'^3}{3k^*}\frac{\partial^2 T'}{\partial y'^2}. \tag{8}$$

With the help of (7) and (8) in expression (6), we have

$$\frac{\partial T'}{\partial t'} = \frac{k_1}{\rho c_p}\frac{\partial^2 T'}{\partial y'^2} + \frac{1}{\rho c_p}\frac{16\sigma^* {T'_\infty}^3}{3k^*}\frac{\partial^2 T'}{\partial y'^2} + \frac{Q_0}{\rho c_p}(T' - T'_\infty). \tag{9}$$

Introducing the quantities free from dimension as follows:

$$y = \frac{U_0 y'}{v}, u = \frac{u'}{U_0}, t = \frac{t' {U_0}^2}{v}, \theta = \frac{(T' - T'_\infty)}{(T'_w - T'_\infty)}, C = \frac{(C' - C'_\infty)}{(C'_w - C'_\infty)}.$$

For simplicity, neglecting the sign "′" from the above expressions, we have:

$$\frac{\partial u}{\partial t} = \left(1 + \frac{1}{\gamma}\right)\frac{\partial^2 u}{\partial y^2} - \left(M^2 + \frac{1}{k}\right)u + G_r\theta + G_m C, \tag{10}$$

$$\frac{\partial \theta}{\partial t} = \frac{1+Nr}{Pr}\frac{\partial^2 \theta}{\partial y^2}, \tag{11}$$

$$\frac{\partial C}{\partial t} = \frac{1}{Sc}\frac{\partial^2 C}{\partial y^2} - Kr\, C. \tag{12}$$

Subject to the beginning and the end constraints:

$$u = \theta = C = 0, y \geq 0, t = 0,$$

$$u = e^{a't}, \theta = 1, C = \begin{cases} t, 0 < t \leq 1 \\ 1, t > 1 \end{cases} = tH(t) - (t-1)H(t-1), y = 0, t > 0,$$

$$u \to 0, \theta \to 0 \ \&\ C \to 0 \quad \text{as } y \to \infty, t > 0. \tag{13}$$

Where $H(t)$ refers to Heaviside's unit-step functions.

$$Gr = \frac{gv\beta'_T(T'_w - T'_\infty)}{{U_0}^3}, M^2 = \frac{\sigma B_0^2\, v}{\rho {U_0}^2}, Gm = \frac{vg\beta'_C(C'_w - C'_\infty)}{{U_0}^3},$$

$$P_r = \frac{\rho v C_p}{k}, Sc = \frac{v}{D_M}, Kr = \frac{v\, k'_2}{{U_0}^2}, \gamma = \frac{\mu_B\sqrt{2\pi_c}}{P_y}, \tau = \frac{\tau}{\rho u^2}.$$

3. Solution

Perfect answer function for liquid movement, temperature and density is calculated for expressions (10) - (12) subject to the constraints (13) by the method of Laplace transform:

$$\theta(y,t) = f_5(y,t), \tag{14}$$

$$C(y,t) = f_9(y,t) - f_9(y,t-1)H(t-1), \tag{15}$$

$$u(y,t) = h_2(y,t) + h_3(y,t) - h_3(y,t-1)H(t-1), \tag{16}$$

where

$$h_2(y,t) = g_1(y,t) + g_5(y,t) - g_7(y,t), \tag{17}$$

$$h_3(y,t) = g_6(y,t) - g_4(y,t), \tag{18}$$

$$g_1(y,t) = \frac{e^{a' t}}{2}\left[e^{-y\sqrt{\frac{1}{a}(b+a')}}\, erfc\,\left(\frac{y}{2\sqrt{a\,t}} - \sqrt{(b+a')t}\right)\right]$$

$$+\frac{e^{a' t}}{2}\left[e^{y\sqrt{\frac{1}{a}(b+a')}}\, erfc\,\left(\frac{y}{2\sqrt{a\,t}} + \sqrt{(b+a')t}\right)\right], \quad (19)$$

$$g_4(y,t) = a_{13}f_8(y,t) + a_{11}f_9(y,t) + a_{12}f_{10}(y,t), \quad (20)$$

$$g_5(y,t) = a_8 f_1(y,t) - a_8 f_3(y,t), \quad (21)$$

$$g_6(y,t) = a_{13}f_1(y,t) + a_{11}f_2(y,t) + a_{12}f_4(y,t), \quad (22)$$

$$g_7(y,s) = a_8 f_5(y,t) - a_8 f_7(y,t), \quad (23)$$

$$f_1(y,t) = \frac{1}{2}\left[e^{-y\sqrt{\frac{b}{a}}}\, erfc\,\left(\frac{y}{2\sqrt{at}} - \sqrt{bt}\right) + e^{y\sqrt{\frac{b}{a}}}\, erfc\,\left(\frac{y}{2\sqrt{at}} + \sqrt{bt}\right)\right], \quad (24)$$

$$f_2(y,t) = \frac{1}{2}\left[\left(t - \frac{y}{2\sqrt{ab}}\right)e^{-y\sqrt{\frac{b}{a}}}\, erfc\,\left(\frac{y}{2\sqrt{at}} - \sqrt{bt}\right)\right]$$

$$+\frac{1}{2}\left[\left(t + \frac{y}{2\sqrt{ab}}\right)e^{y\sqrt{\frac{b}{a}}}\, erfc\,\left(\frac{y}{2\sqrt{at}} + \sqrt{bt}\right)\right], \quad (25)$$

$$f_3(y,t) = \frac{e^{a_2 t}}{2}\left[e^{-y\sqrt{\frac{1}{a}(b+a_2)}}\, erfc\,\left(\frac{y}{2\sqrt{a\,t}} - \sqrt{(b+a_2)t}\right)\right]$$

$$+\frac{e^{a_2 t}}{2}\left[e^{y\sqrt{\frac{1}{a}(b+a_2)}}\, erfc\,\left(\frac{y}{2\sqrt{a\,t}} + \sqrt{(b+a_2)t}\right)\right], \quad (26)$$

$$f_4(y,t) = \frac{e^{-a_6 t}}{2}\left[e^{-y\sqrt{\frac{1}{a}(b-a_6)}}\, erfc\,\left(\frac{y}{2\sqrt{a\,t}} - \sqrt{(b-a_6)t}\right)\right]$$

$$+\frac{e^{-a_6 t}}{2}\left[e^{y\sqrt{\frac{1}{a}(b-a_6)}}\, erfc\,\left(\frac{y}{2\sqrt{a\,t}} + \sqrt{(b-a_6)t}\right)\right], \quad (27)$$

$$f_5(y,t) = erfc\,\left(\frac{y}{2\sqrt{d\,t}}\right), \quad (28)$$

$$f_7(y,t) = \frac{e^{a_2\,t}}{2}\left[e^{-y\sqrt{a_2/d}}\, erfc\,\left(\frac{y}{2\sqrt{d\,t}} - \sqrt{a_2 t}\right) + e^{y\sqrt{a_2/d}}\, erfc\,\left(\frac{y}{2\sqrt{d\,t}} + \sqrt{a_2 t}\right)\right], \quad (29)$$

$$f_8(y,t) = \frac{1}{2}\left[e^{-y\sqrt{Kr\,Sc}}\, erfc\,\left(\frac{y\sqrt{Sc}}{2\sqrt{t}} - \sqrt{Kr\,t}\right)\right]$$

$$+\frac{1}{2}\left[e^{y\sqrt{Kr\,Sc}}\, erfc\,\left(\frac{y\sqrt{Sc}}{2\sqrt{t}} + \sqrt{Kr\,t}\right)\right], \quad (30)$$

$$f_9(y,t) = \frac{1}{2}\left[\left(t - \frac{y\sqrt{Sc}}{2\sqrt{Kr}}\right)e^{-y\sqrt{Sc\,Kr}}\, erfc\,\left(\frac{y\sqrt{Sc}}{2\sqrt{t}} - \sqrt{Kr\,t}\right)\right]$$

$$+\frac{1}{2}\left[\left(t+\frac{y\sqrt{Sc}}{2\sqrt{Kr}}\right)e^{y\sqrt{Sc\,Kr}}\ erfc\ \left(\frac{y\sqrt{Sc}}{2\sqrt{t}}+\sqrt{Kr\,t}\right)\right], \tag{31}$$

$$f_{10}(y,t)=\frac{e^{-a_6 t}}{2}\left[e^{-y\sqrt{Sc(Kr-a_6)}}\ erfc\ \left(\frac{y\sqrt{Sc}}{2\sqrt{t}}-\sqrt{(Kr-a_6)t}\right)\right]$$

$$+\frac{e^{-a_6 t}}{2}\left[e^{y\sqrt{Sc(Kr-a_6)}}\ erfc\ \left(\frac{y\sqrt{Sc}}{2\sqrt{t}}+\sqrt{(Kr-a_6)t}\right)\right]. \tag{32}$$

4. Skin friction, Nusselt number, and Sherwood number

The formula for N_u is calculated from equation (14) using the relation,

$$N_u=-\left(\frac{\partial\theta}{\partial y}\right)_{y=0}, \tag{33}$$

$$N_u=-[I_5(t)]\ . \tag{34}$$

Expressions of S_h can be obtained from equation (15) with the help of

$$S_h=-\left(\frac{\partial C}{\partial y}\right)_{y=0}, \tag{35}$$

$$S_h=-[I_9(t)-I_9(t-1)H(t-1)]. \tag{36}$$

Format of skin friction can be obtained from equation (16) with the help of

$$\tau^*(y,t)=-\mu_B\left(1+\frac{1}{\gamma}\right)\tau, \tag{37}$$

Here, $\tau=\frac{\partial u}{\partial y}|_{y=0}$, (38)

$$\tau=I_{19}(t)+I_{20}(t)-I_{20}(t-1)H(t-1), \tag{39}$$

where

$$I_1(t)=-\sqrt{\frac{b}{a}}\left(\sqrt{bt}\right)-\frac{e^{-bt}}{\sqrt{\pi a t}}, \tag{40}$$

$$I_2(t)=-\frac{1}{\sqrt{4ab}}\left(\sqrt{bt}\right)-t\sqrt{\frac{b}{a}}\left(\sqrt{bt}\right)-\frac{t\,e^{-bt}}{\sqrt{\pi a t}}, \tag{41}$$

$$I_3(t)=-e^{a_2 t}\sqrt{\frac{b+a_2}{a}}\left(\sqrt{(b+a_2)t}\right)-\frac{e^{-bt}}{\sqrt{\pi a t}}, \tag{42}$$

$$I_4(t)=-e^{-a_6 t}\sqrt{\frac{b-a_6}{a}}\left(\sqrt{(b-a_6)t}\right)-\frac{e^{-bt}}{\sqrt{\pi a t}}, \tag{43}$$

$$I_5(t)=-\sqrt{\frac{1}{\pi t d}}, \tag{44}$$

$$I_7(t)=-e^{a_2 t}\sqrt{a_2/d}\left(\sqrt{a_2 t}\right)-\sqrt{\frac{1}{d\,\pi t}}, \tag{45}$$

$$I_8(t)=-\sqrt{Kr\,Sc}\left(\sqrt{Kr\,t}\right)-\sqrt{\frac{Sc}{\pi t}}e^{-Kr\,t}, \tag{46}$$

$$I_9(t) = -\sqrt{\frac{Sc}{4\,Kr}}\left(\sqrt{Kr\,t}\right) - t\sqrt{Sc\,Kr}\left(\sqrt{Kr\,t}\right) - \sqrt{\frac{t\,Sc}{\pi}}e^{-Kr\,t}, \tag{47}$$

$$I_{10}(t) = -e^{-a_6 t}\sqrt{Sc(Kr-a_6)}\left(\sqrt{(Kr-a_6)t}\right) - \sqrt{\frac{Sc}{\pi t}}\,e^{-\,Kr\,t}, \tag{48}$$

$$I_{11}(t) = -e^{a' t}\sqrt{\frac{b+a'}{a}}\left(\sqrt{(b+a')t}\right) - \frac{e^{-bt}}{\sqrt{\pi a t}}, \tag{49}$$

$$I_{14}(t) = a_{13}I_8(t) + a_{11}I_9(t) + a_{12}I_{10}(t), \tag{50}$$

$$I_{15}(t) = a_8 I_1(t) - a_8 I_3(t), \tag{51}$$

$$I_{16}(t) = a_{13}I_1(t) + a_{11}I_2(t) + a_{12}I_4(t), \tag{52}$$

$$I_{17}(t) = a_8 I_5(t) - a_8 I_7(t), \tag{53}$$

$$I_{19}(t) = I_{11}(t) + I_{15}(t) - I_{17}(t), \tag{54}$$

$$I_{20}(t) = I_{16}(t) - I_{14}(t). \tag{55}$$

5. Result and discussion

Figure 2 states that when Gamma (Casson Parameter) gets increased, velocity goes down. Physically, the Plasticity of fluid will be improved by decreasing the value of the Casson fluid parameter. Due to this reason, velocity boundary thickness will improve. Figure 3 states that the magnetic field is negatively correlated with velocity. From Figure 4, it is clear that the temperature will go down when we increase the Prandtl number. This result agrees with the fact that the Prandtl number tends to reduce the thermal conductivity of the fluid. From Figure 5, it is clear that Schmidt number is negatively correlated with the concentration. Figures 6 and 7 state the effect of mass and thermal Grashof number on velocity profiles, respectively. From Figure 6, it is seen that when the mass Grashof number is increased, velocity will also increase. Figure 7 shows that the thermal Grashof number and Velocity are Positively Correlated. Figure 8 shows that when we increase the Chemical reaction value, the concentration decreases. This shows that Kr > 0 leads to a reduction in the concentration field. This result is strongly in agreement with physical realities. From Figure 9, it is clear that the Heating Profile has an upward tendency when we increase the thermal radiation parameter. Figure 10 shows the effects of porosity on velocity profiles. It is illustrated that the porous medium parameter tends to improve the motion of the fluid.

6. Conclusion

- When the Casson Parameter and Magnetic field rise, the Velocity Profile tends to fall.
- When the Grashof numbers for heat, mass transfer, and thermal conductivity increase, the Velocity Profile tends to increase as well.
- When the species of chemical and the Schmidt Number go up, the concentration is prone to decrease.
- The property related to temperature seems to get lower as the Prandtl number grows.

References

Brewster, M. Q. (1972). *Thermal Radiative Transfer Properties*, John Wiley and Sons, Chichester.

Casson, N. (1957). A flow equation for the pigment oil suspensions of the printing ink type, C.C. Mills (Ed.), Rheology of Disperse Systems, Pergamon, New York Oxford, pp. 84-104.

Deo, S. and Kumar, S. (2021). (R1471) MHD Reiner-Rivlin Liquid Flow through a Porous Cylindrical Annulus, Applications and Applied Mathematics: An International Journal (AAM), Vol. 16, Iss. 2, Article 15.

Divya, B. B., Manjunatha, G., Rajashekhar, C., Vaidya, H. and Prasad, K.V. (2020). Analysis of temperature-dependent properties of a peristaltic MHD flow in a non-uniform channel: A Casson fluid model, Latin American Applied Research Pesquisa Aplicada Latino Americana, Vol. 50, No. 03, pp. 151-158.

Hartmann, J. (1937). Hg-dynamics-I theory of the laminar flow of an electrically conductive liquid in a homogenous magnetic field, Det Kal. Danske Videnskabernes Selskab, Mathematisk-Fysiske Meddeleser, Vol. 15, pp. 1–27.

Kataria, H and Mittal, A. (2015). Mathematical model for velocity and temperature of gravity-driven convective optically thick nanofluid flow past an oscillating vertical plate in the presence of magnetic field and radiation, J. Niger. Mathematical Society, Vol. 34, pp. 303-317.

Prameela, M., Gangadhar, K. and Reddy, G.J. (2022). MHD free convective non-Newtonian Casson fluid flow over an oscillating vertical plate, Partial Differential Equations in Applied Mathematics, Vol. 5, Article 100366.

Rajput, U. S. and Kumar, G. (2016). Unsteady MHD Flow Past an Impulsively Started Inclined Plate with Variable Temperature and Mass Diffusion in the presence of Hall current, Applications, and Applied Mathematics: An International Journal (AAM), Vol. 11, Iss. 2, Article 13.

Rajput, U. S., and Gupta, N.K. (2021). Hall Current and Radiation Effects on Unsteady Natural Convection MHD flow with Inclined Magnetic field, Applications, and Applied Mathematics: An International Journal (AAM), Vol. 16, Iss. 1, Article 29.

Ramalingeswara Rao, S., Vidyasagar, G. and Deekshitulu, G.V.S.R. (2020). Unsteady MHD free convection Casson fluid flow past an exponentially accelerated infinite vertical porous plate through a porous medium in the presence of radiation absorption with heat generation/absorption, Materials Today: Proceedings, Vol. 42, No. 1.

Ramesh, G. K., Ganesh Kumar, K., Shehzad, S. A. and Gireesha, B. J. (2018). Enhancement of radiation on hydromagnetic Casson fluid flow towards a stretched cylinder with suspension of liquid particles, Canadian Jour. of Phy., Vol. 96, pp. 18-24.

Prabhakar Reddy, B., Makinde, O. D. and Hugo, A. (2022). A computational study on diffusion-thermo and rotation effects on heat generated mixed convection flow of MHD Casson fluid past an oscillating porous plate, International Communications in Heat and Mass Transfer, Vol. 138, Article 106389.

Vaddemani, R.R., Kodi, R. and Mopuri, O. (2021). Characteristics of MHD Casson fluid past an inclined vertical porous plate, Materials Today: Proceedings, Vol. 49, No. 5, pp. 2136-2142.

Veera Krishna, M. (2022). Chemical reaction, heat absorption and Newtonian heating on MHD free convective Casson hybrid nanofluids past an infinite oscillating Vertical porous plate, International Communications in Heat and Mass Transfer, Vol. 138, Article 106327.

APPENDIX A

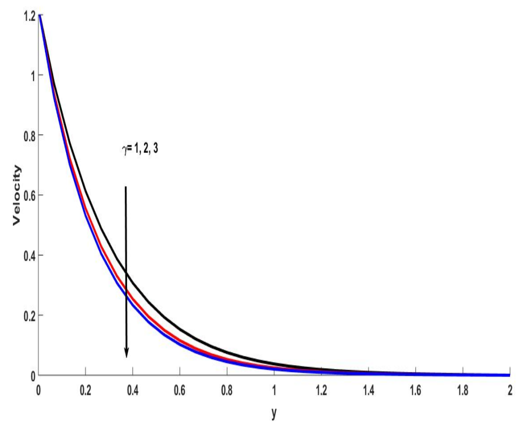

Figure 2. Velocity for different values of γ

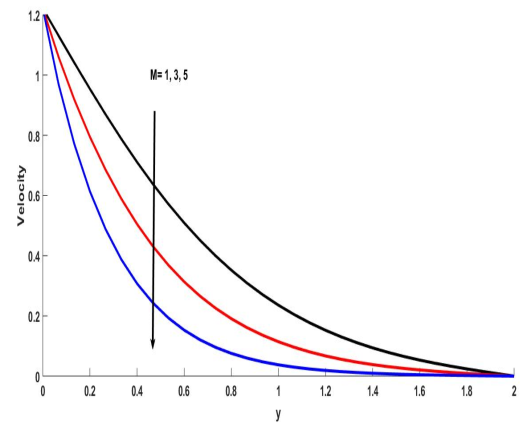

Figure 3. Velocity for different values of M

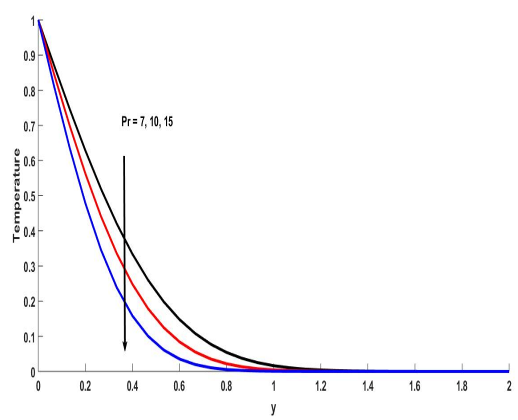

Figure 4. Temperature for different values of Pr

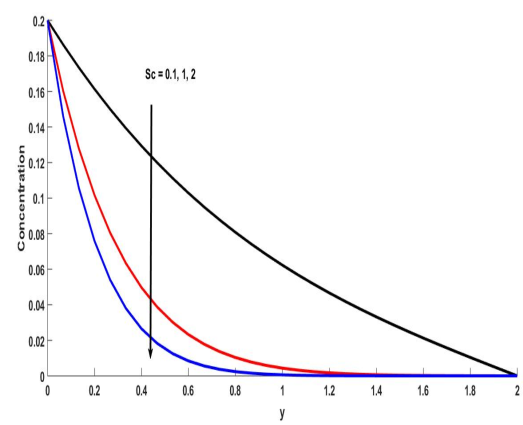

Figure 5. Concentration for different values of Sc

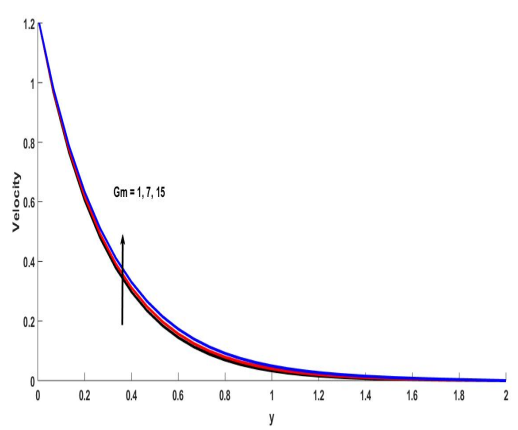

Figure 6. Velocity for different values of Gm

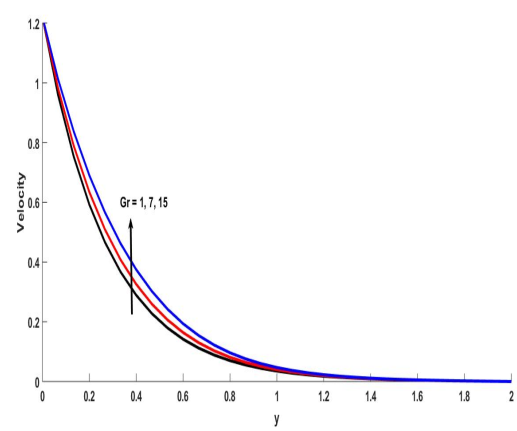

Figure 7. Velocity for different values of Gr

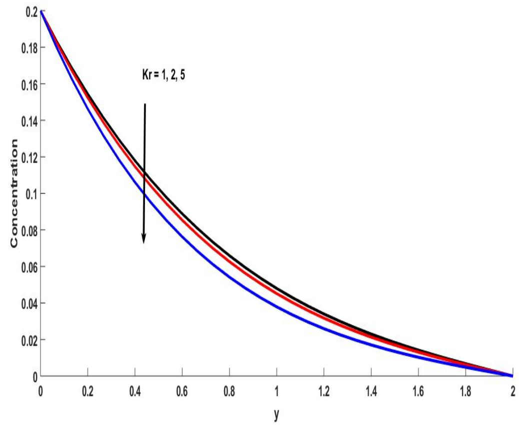

Figure 8. Concentration for different values of Kr

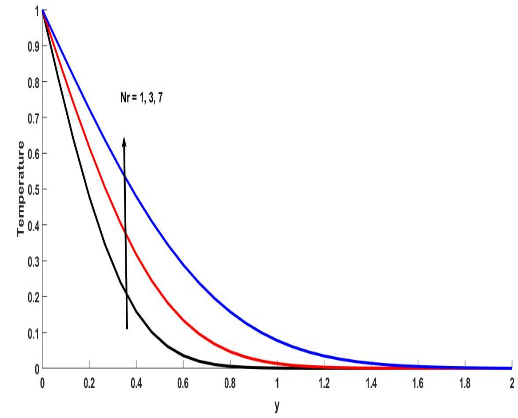

Figure 9. Temperature for different values of Nr

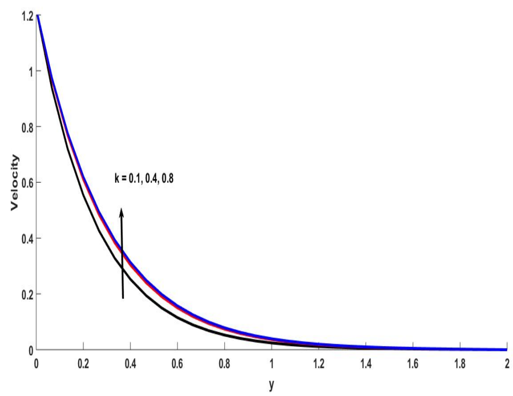

Figure 10. Velocity for different values of k

APPENDIX B

$a = 1 + \frac{1}{\gamma}$	$b = M^2 + \frac{1}{k}$	$d = \frac{1+Nr}{Pr}$
$a_1 = \frac{a}{d} - 1$	$a_2 = \frac{b}{a_1}$	$a_3 = \frac{Gr}{a_1}$
$a_4 = a\, Sc - 1$	$a_5 = a\, Sc\, Kr - b$	$a_6 = \frac{a_5}{a_4}$
$a_7 = \frac{Gm}{a_4}$	$a_8 = -\frac{a_3}{a_2}$	$a_9 = \frac{a_3}{{a_2}^2}$
$a_{10} = \frac{a_3}{(1-a_2)} - a_8 - \frac{a_9}{(1-a_2)}$	$a_{11} = \frac{a_7}{a_6}$	$a_{12} = \frac{a_7}{{a_6}^2}$
$a_{13} = \frac{a_7}{(1+a_6)} - a_{11} - \frac{a_{12}}{(1+a_6)}$	$H_2(y,s) = G_1(y,s) + G_5(y,s) - G_7(y,s)$	$H_3(y,s) = G_6(y,s) - G_4(y,s)$

$G_1(y,s) = \frac{1}{s-a'} e^{-y\sqrt{\frac{s+b}{a}}}$	$G_5(y,s) = a_8 F_1(y,s) - a_8 F_3(y,s)$	$G_6(y,s) = a_{13} F_1(y,s) + a_{11} F_2(y,s) + a_{12} F_4(y,s)$
$G_4(y,s) = a_{13} F_8(y,s) + a_{11} F_9(y,s) + a_{12} F_{10}(y,s)$	$F_1(y,s) = \frac{1}{s} e^{-y\sqrt{\frac{s+b}{a}}}$	$F_2(y,s) = \frac{1}{s^2} e^{-y\sqrt{\frac{s+b}{a}}}$
$G_7(y,s) = a_8 F_5(y,s) - a_8 F_7(y,s)$	$F_4(y,s) = \frac{1}{(s+a_6)} e^{-y\sqrt{\frac{s+b}{a}}}$	$F_5(y,s) = \frac{1}{s} e^{-y\sqrt{\frac{s}{d}}}$
$F_3(y,s) = \frac{1}{(s-a_2)} e^{-y\sqrt{\frac{s+b}{a}}}$	$F_7(y,s) = \frac{e^{-y\sqrt{\frac{s}{d}}}}{(s-a_2)}$	$F_8(y,s) = \frac{1}{s} e^{-y\sqrt{Sc\,(Kr+s)}}$
$F_9(y,s) = \frac{1}{s^2} e^{-y\sqrt{Sc\,(Kr+s)}}$	$F_{10}(y,s) = \frac{e^{-y\sqrt{Sc\,(Kr+s)}}}{(s+a_6)}$	$f_i(y,t) = L^{-1}\big(F_i(y,s)\big)$, For $i = 1\ to\ 5\ \&\ 7\ to\ 10$
$g_i(y,t) = L^{-1}\big(G_i(y,s)\big)$, For $i = 1\ \&\ 4\ to\ 7$	$h_i(y,t) = L^{-1}\big(H_i(y,s)\big)$, For $i = 2\ \&\ 3$	$I_i = \frac{df_i}{dy}\Big\vert_{y=0}$, For $i = 1\ to\ 5\ \&\ 7\ to 10$
$I_{i=1\,1\,\&\,14\ to\,17} = \frac{dg_j}{dy}\Big\vert_{y=0}$, For $j = 1\ \&\ 4\ to\ 7$	$I_{i=1\,9\,\&\,20} = \frac{dh_j}{dy}\Big\vert_{y=0}$, For $j = 2\ \&\ 3$	